A 100-Gb/s noncoherent silicon receiver for PDM-DBPSK/DQPSK signals

Jonathan Klamkin,[1,2,*] Fabrizio Gambini,[3] Stefano Faralli,[2] Antonio Malacarne,[3] Gianluca Meloni,[3] Gianluca Berrettini,[2] Giampiero Contestabile,[2] and Luca Potì[3]

[1]*Electrical and Computer Engineering Department, Boston University, Boston, Massachusetts 02215, USA*
[2]*Scuola Superiore Sant'Anna, 56124 Pisa, Italy*
[3]*CNIT, Photonic Networks National Lab, 56124 Pisa, Italy*
[*]*klamkin@bu.edu*

Abstract: An integrated noncoherent silicon receiver for demodulation of 100-Gb/s polarization-division multiplexed differential quadrature phase-shift keying and polarization-division multiplexed differential binary phase-shift keying signals is demonstrated. The receiver consists of a 2D surface grating coupler, four Mach-Zehnder delay interferometers and four germanium balanced photodetectors.

OCIS codes: (130.0130) Integrated optics; (130.3120) Integrated optics devices; (060.5060) Phase modulation; (060.2330) Fiber optics communications.

References and links

1. M. A. Taubenblatt, "Optical interconnects for high-performance computing," J. Lightwave Technol. **30**(4), 448–457 (2012).
2. C. Gunn, "CMOS photonics for high-speed interconnects," IEEE Micro **26**(2), 58–66 (2006).
3. C. R. Doerr, N. K. Fontaine, and L. L. Buhl, "PDM-DQPSK silicon receiver with integrated monitor and minimum number of controls," IEEE Photon. Technol. Lett. **24**(8), 697–699 (2012).
4. P. Dong, L. Chen, C. Xie, L. L. Buhl, and Y.-K. Chen, "50-Gb/s silicon quadrature phase-shift keying modulator," Opt. Express **20**(19), 21181–21186 (2012).
5. P. Dumon, W. Boegarts, V. Wiaux, J. Wouters, S. Beckx, J. Van Campenhout, D. Taillaert, B. Luyassert, P. Bientsman, D. Van Thourhourt, and R. Baets, "Low-loss SOI photonic wires and ring resonators fabricated with deep UV lithography," IEEE Photon. Technol. Lett. **16**(5), 1328–1330 (2004).
6. A. Novack, Y. Liu, R. Ding, M. Gould, T. Baehr-Jones, Q. Li, Y. Yang, Y. Ma, Y. Zhang, K. Padmaraju, K. Bergman, A. E.-J. Lim, G.-Q. Lo, and M. Hochberg, "A 30 GHz silicon photonics platform," Proc. SPIE **8781**, 878107 (2013).
7. P. J. Winzer and R.-J. Essiambre, "Advanced modulation formats for high-capacity optical transport networks," J. Lightwave Technol. **24**(12), 4711–4728 (2006).
8. C. R. Doerr, P. J. Winzer, Y.-K. Chen, S. Chandrasekhar, M. S. Rasras, L. Chen, T.-Y. Liow, K.-W. Ang, and G.-Q. Lo, "Monolithic polarization and phase diversity coherent receiver in silicon," J. Lightwave Technol. **28**(4), 520–525 (2010).
9. Y. Painchaud, M. Pelletier, M. Poulin, F. Pelletier, C. Latrasse, G. Robidoux, S. Savard, J.-F. Gagné, V. Trudel, M.-J. Picard, P. Poulin, P. Sirois, F. D'Amours, D. Asselin, S. Paquet, C. Paquet, M. Cur, M. Guy, M. Morsy-Osman, Q. Zhuge, X. Xu, M. Chagnon, and D. V. Plant, "Ultra-compact coherent receiver based on hybrid integration on silicon," in Proc. OFC, paper OM2J.2, Anaheim, CA (2013).
10. B. Mikkelsen, "Challenges and key technologies for coherent metro 100G transceivers," Lightwave Magazine, 14–18 (NOV/DEC 2012).
11. A. H. Gnauck and P. J. Winzer, "Optical phase-shift-keyed transmission," J. Lightwave Technol. **23**(1), 115–130 (2005).
12. R. A. Griffin and A. C. Carter, "Optical differential quadrature phase-shift key (oDQPSK) for high capacity optical transmission," in Proc. OFC, paper WX6, Anaheim, CA (2002).
13. C. R. Doerr, L. Zhang, L. L. Buhl, J. H. Sinsky, A. H. Gnauck, P. J. Winzer, A. L. Adamiecki, and N. J. Sauer, "High-speed InP DQPSK receiver," in Proc. OFC, paper PDP23, San Diego, CA (2008).
14. L. Zimmermann, K. Voigt, G. Winzer, and K. Petermann, "Towards silicon on insulator dqpsk demodulators," in Proc. OFC, paper OThB3, San Diego, CA (2010).
15. S. Faralli, K. N. Nguyen, J. D. Peters, D. T. Spencer, D. J. Blumenthal, and J. E. Bowers, "Integrated hybrid Si/InGaAs 50 Gb/s DQPSK receiver," Opt. Express **20**(18), 19726–19734 (2012).
16. K. Xu, Z. Cheng, C. Y. Wong, and H. K. Tsang, "Tunable integrated variable bit-rate DPSK silicon receiver," Opt. Lett. **37**(22), 4738–4740 (2012).
17. F. Gambini, S. Faralli, A. Malacarne, G. Meloni, G. Berrettini, G. Contestabile, L. Potì, and J. Klamkin, "A Silicon receiver for 100 Gb/s PDM-DQPSK signals," in Proc. Photonics in Switching Conference, paper PD2–1, Kyoto, Japan (2013).

#202125 - $15.00 USD Received 28 Nov 2013; revised 12 Jan 2014; accepted 13 Jan 2014; published 24 Jan 2014

18. D. Taillaert, H. Chong, P. I. Borel, L. H. Frandsen, R. M. De La Rue, and R. Baets, "A compact two-dimensional grating coupler used as a polarization splitter," IEEE Photon. Technol. Lett. **15**(9), 1249–1251 (2003).
19. S. Spector, M. W. Geis, D. Lennon, R. C. Williamson, and T. M. Lyszczarz, "Hybrid multi-mode/single-mode waveguides for low loss," in Proc. Integrated Photonics Research Conference, paper IThE5, San Francisco, CA (2004).
20. H. Kim and P. J. Winzer, "Robustness to laser frequency offset in direct-detection DPSK and DQPSK systems," J. Lightwave Technol. **21**(9), 1887–1891 (2003).

1. Introduction

Silicon (Si) photonics has become a viable technology for reducing the size, weight and power of transceivers for short-reach optical interconnects and optical fiber transmission systems [1–4]. This technology promises low-cost and high-volume production, complimentary metal-oxide-semiconductor (CMOS) compatibility and potential for monolithic integration with electronics. The most widely developed platform utilizes Si-on-insulator (SOI) nanowire waveguides [5], and recently this platform has been extended to include integrated active components such as modulators and photodetectors [6].

For increasing spectral efficiency in optical fiber transmission systems, advanced modulation formats have been proposed and demonstrated. Using coherent detection techniques, such systems can yield improved receiver sensitivity and can compensate for chromatic dispersion and nonlinearities using digital post processing [7]. Because of the complexity of transmitters and receivers for such systems, it is expected that photonic integration will play a major role. Therefore a number of demonstrations of photonic integrated circuits (PICs) have been reported including a polarization and phase diversity coherent receiver in Si [8]. This PIC was tested for receiving polarization-division multiplexed quadrature phase-shift keying (PDM-QPSK) signals up to 112 Gb/s. In other work, an ultra-compact coherent receiver was developed using hybrid integration of a photodetector array and transimpedance amplifiers with Si passive components. With this receiver, transmission of 28 Gbaud PDM-QPSK signals up to 4,800 km was demonstrated [9].

Although coherent detection allows for full recovery of amplitude, phase, and polarization, the application specific integrated circuits (ASICs) required for digital signal processing (DSP) consume significant power. To make coherent detection viable for use in metro networks where size and power consumption requirements are more stringent than for long-haul networks, ultra-low power ASICs have been proposed [10]. An alternative, which would make QPSK signals suitable for short- and medium-reach links, is to use noncoherent detection techniques that allow for demodulation of advanced modulation format signals without complex DSP or a local oscillator laser [3, 11]. Differential QPSK (DQPSK) is a multi-level phase modulation format that was proposed for use with a self-homodyne direct detection scheme [12]. This modulation format has an enhanced spectral efficiency compared to binary on-off keying (OOK) while not requiring coherent detection and DSP. To use conventional square-law photodetection, phase to intensity conversion components are required. Delay interferometers (DI) can be used so that each bit provides a phase reference for another bit [7]. The differential delay is set to the symbol duration so that neighboring bits interfere upon combination at the output of a Mach-Zehnder (MZ)-DI and thus the phase-encoded data is converted to intensity data that depends on the phase difference between adjacent bits.

As for other advanced modulation format transceivers, PICs are attractive for reducing size and power consumption as well as cost for DQPSK-based systems. An indium phosphide

#202125 - $15.00 USD Received 28 Nov 2013; revised 12 Jan 2014; accepted 13 Jan 2014; published 24 Jan 2014

Table 1. Summary of Reported Direct Detection Advanced Modulation Format Receivers

Modulation format	Integration platform	Maximum bit rate	Footprint	Reference
DQPSK	InP	107 Gb/s	3.2 x 0.8 mm^2	[13]
DPSK	Si	12.5 Gb/s	NA	[16]
PDM-DQPSK	Si	43 Gb/s	6.7 x 1.8 mm^2	[3]
DQPSK	Hybrid (InP/Si)	50 Gb/s	3.5 x 1.8 mm^2	[15]
PDM-DBPSK/DQPSK	Si	100 Gb/s	3.0 x 1.0 mm^2	This work

(InP)-based PIC DQPSK receiver demonstrated 107 Gb/s operation and a footprint of 3.2 x 0.8 mm^2 [13]. For realizing such a receiver in Si, the authors in [14] developed demodulator structures in SOI technology while closely addressing polarization issues. In [3], a PDM-DQPSK receiver was demonstrated in Si up to 43 Gb/s with a footprint of 6.7 x 1.8 mm^2 and in [15] a hybrid Si DQPSK receiver was demonstrated up to 50 Gb/s with a footprint of 3.5 x 1.8 mm^2. To extend the wavelength operating range and increase the bit-rate scalability, Si microring resonators were proposed in [16] and demonstrated up to 12.5 Gb/s operation for DPSK signals. The footprint is not provided but is expected to be small. In this work, a Si receiver is demonstrated for PDM-DQPSK and PDM- differential binary phase-shift keying (DBPSK) signals. The receiver operates up to 100 Gb/s. Preliminary results were presented in [17] for PDM-DQPSK signals. The receiver consists of a 2D surface grating coupler used for polarization splitting and rotation, four MZ-DIs with phase shifters and four germanium (Ge) balanced photodetectors with integrated metal-insulator-metal (MIM) capacitors. The capacitance of the MIM capacitors is approximately 1.2 pF. The receiver footprint is 3 x 1 mm^2. The receiver can be employed for 25 Gbaud PDM-DQPSK signals (thus 100 Gb/s) and also for polarization-insensitive DQPSK. Table 1 displays a summary of reported direct detection advanced modulation format receivers that are based on MZ-DIs.

2. Device design and characterization

A schematic of the receiver and a mask layout of are shown in Fig. 1. The circuit was fabricated at the Institute of Microelectronics (IME), Singapore, through the OpSIS (Optoelectronic Systems Integration in Silicon) foundry. It was realized with a 220-nm thick SOI technology where the buried oxide layer has a thickness of 2 μm. Single-mode strip waveguides are 500-nm wide and the minimum bending radius used for the integrated receiver was 5 μm, which yields extremely low bend loss.

The 2D grating coupler is used to couple the optical signal from a fiber to the chip and also to split the polarization multiplexed signal into separate TE waveguides [18]. The coupler therefore also serves as a polarization rotator for TM light, which is beneficial in that all of the chip components are designed for a single polarization. The light from each polarization is also split in a forward and backward direction where one side is connected to the MZ-DIs and the other side is connected to a monitor Ge photodiode (PD). If the fiber is vertical to the chip, the light from each polarization is split into a ratio of 50:50 by the grating coupler. If the fiber is inclined at an angle other than 90° with respect to the chip, the splitting ratio will vary differently for each polarization. This could, however, be accounted for in using the PDs to monitor the polarization of the incoming signal. The extinction ratio (ER) of the polarization splitter was measured using these monitor PDs and the results are shown in Fig. 2. The input polarization was adjusted using a polarization controller (PC) in order to maximize the photocurrent measured at the 2D grating coupler X port, and the photocurrent was recorded for both the X and Y ports. The same measurements were performed for photocurrent maximized at the Y port. The extinction ratio for the X port ($ER_{X,Y}$) was between 11 and 21 dB for a wavelength range of 1540-1570 nm. That for the Y port ($ER_{Y,X}$) was 15-24 dB.

#202125 - $15.00 USD Received 28 Nov 2013; revised 12 Jan 2014; accepted 13 Jan 2014; published 24 Jan 2014

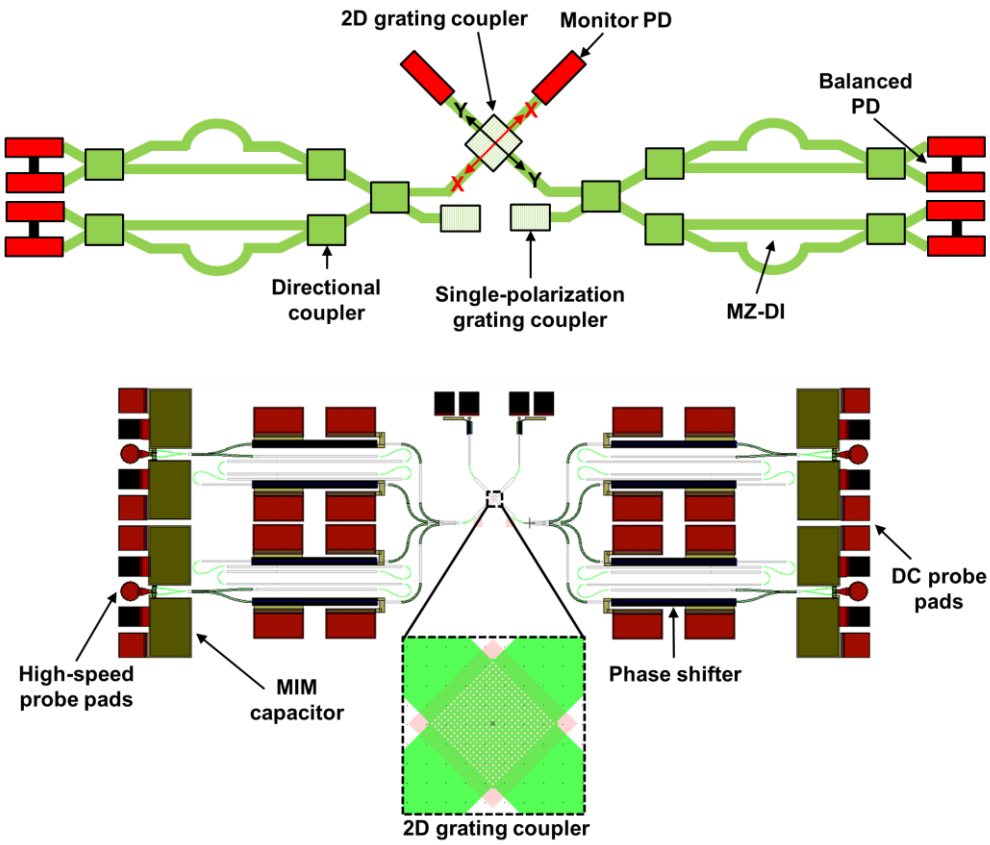

Fig. 1. Schematic (top) and mask layout (bottom) of integrated Si PDM-DBPSK/DQPSK receiver. A close-up of the layout of the 2D grating coupler is shown.

The MZ-DIs, which are used to convert differential phase modulation into intensity modulation, are constructed using both rib and strip waveguides to realize a compact structure with low insertion loss. Rib waveguides are used for long straight sections and strip waveguides are used for curved sections, inspired by the architecture presented in [19]. For splitting and combining functions, directional couplers are used. The group indices of the rib and strip waveguides determined from finite-difference time domain simulations are 3.88 and 4.17 respectively at a wavelength of 1.55 μm. The hybrid rib/strip MZ-DI was intended to have a differential delay of 40 ps, corresponding to a 1 bit delay for a baud rate of 25 Gbaud. There was however some inaccuracy in the simulations used for determining the group indices during the design of the receiver, which underestimated the group indices. Therefore as shown in the spectrum in Fig. 3, the measured FSR was 23 GHz instead of 25 GHz. This could be corrected for in future implementations and does in any way limit the manufacturability of the receiver. The measurement was performed using a separate test structure that has the identical MZ-DI design but has an optical input and optical output, both realized with single-polarization (TE) grating couplers. A continuous wave TE-polarized signal was coupled to the input grating coupler and the spectrum of the interfered wave was observed using and optical spectrum analyzer. The thermal phase shifters incorporated into each branch of each MZ-DI can be used to fine tune the MZI-DI filters. These phase shifters are realized with resistive heaters and each phase shifter is 500 μm long. They can be used to increase design and fabrication tolerance. It was suggested in [20] that if an active control loop were incorporated to continuously tune the DI, it should have a bandwidth exceeding

#202125 - $15.00 USD Received 28 Nov 2013; revised 12 Jan 2014; accepted 13 Jan 2014; published 24 Jan 2014

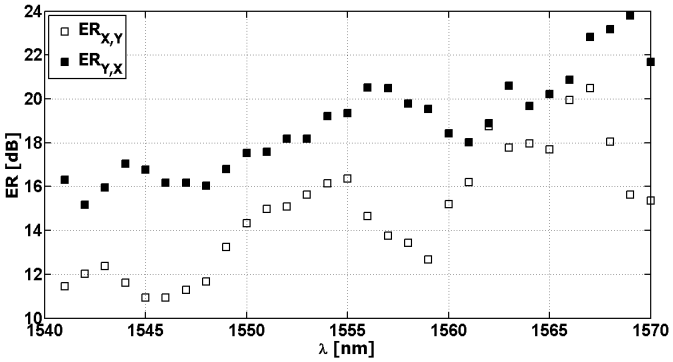

Fig. 2. ER for the X and Y ports of the 2D grating coupler.

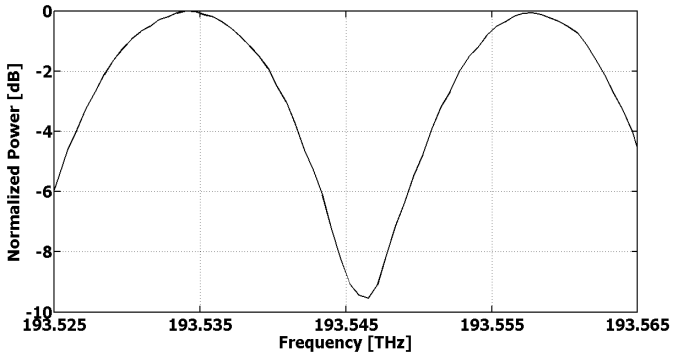

Fig. 3. Spectral response of MZ-DI.

several kHz. The integrated thermal heaters used in this work for phase tuning can operate in the MHz range and therefore meet this requirement. In a real-time system, they could also be used to fine tune the delay using a feedback control circuit to reduce the frequency mismatch between the laser source and MZ-DI.

In total there are four balanced Ge photodetectors, two for each polarization. Each balanced pair consists of two Ge PDs that are connected in series and each are connected to an on-chip MIM capacitor for DC decoupling. High speed ground-signal-ground probe pads are used to extract the data signals from the chip and slightly larger probe pads are used for DC biasing. All of these pads are positioned in a linear fashion near the edge of the receiver circuit, so that a combined RF/DC multiprobe can be used. Typical responsivity, dark current, and 3-dB bandwidth of single photodetectors are 0.55 A/W, 5 μA (at 4 V reverse bias) and 20 GHz respectively. The bandwidth of each photodetector in a balanced pair appears to be significantly lower, on the order of 10 GHz. This is due to a fabrication error resulting in higher than expected device resistance and can be improved in future implementations.

3. Receiver results and discussion

To characterize the performance of the receiver, the experimental setup shown in Fig. 4 was used. A transmitter with a DFB laser operating at 1548 nm modulated by a nested Mach-Zehnder I-Q modulator was used to generate a variable symbol rate DBPSK or DQPSK signal with a pseudo random binary sequence (PRBS). The signal was amplified by an erbium-doped fiber amplifier (EDFA) and then combined with a filtered amplified spontaneous emission (ASE) source in order to vary the optical signal to noise ratio (OSNR). The signal was filtered and polarization controlled before being coupled to the PDM-DQPSK receiver PIC. The receiver can be operated for polarization multiplexed signals using the 2D grating

#202125 - $15.00 USD Received 28 Nov 2013; revised 12 Jan 2014; accepted 13 Jan 2014; published 24 Jan 2014

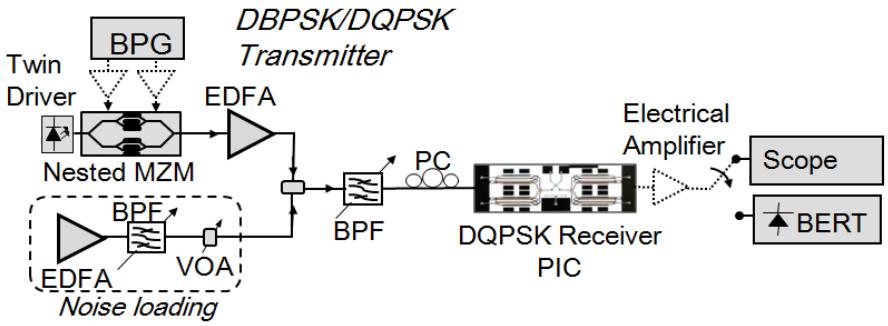

Fig. 4. Experimental measurement setup (BPG = bit pattern generation, MZM = Mach-Zehnder modulator, EDFA = erbium-doped fiber amplifier, BERT = bit error rate tester, BPF = band pass filter, VOA = variable optical attenuator).

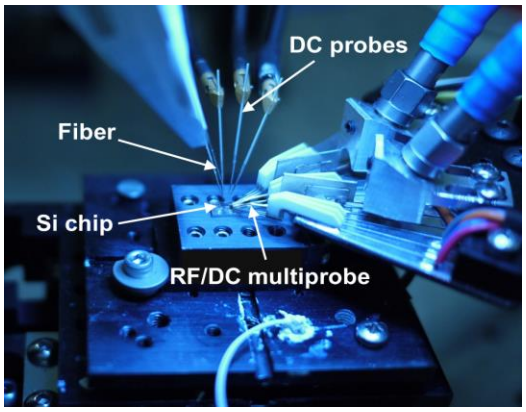

Fig. 5. Photograph of receiver under test.

coupler as described. The 2D grating coupler demonstrates a high coupling loss of approximately 18 dB, and a large fraction of this loss is due to the tapers that have not been optimized. It is anticipated that the coupling loss could be significantly improved in future implementations. The receiver has two additional single-polarization grating couplers that are connected to each pair of MZ-DIs so that each side of the receiver could be operated separately with a single polarization. The coupling loss of the single-polarization grating couplers is approximately 5 dB. The RF signals are collected from the balanced photodetectors through a multiprobe array and are then amplified with low noise electrical amplifiers prior to analysis. A photograph of the setup is shown in Fig. 5. For ease of visualization the multiprobe array for only one side is shown. Separate DC probes are used for the monitor photodetectors and for the phase shifter heaters. The signals can be analyzed alternatively by a sampling oscilloscope or by an error analyzer for bit error rate (BER) measurements.

The receiver was firstly characterized for DBPSK signals. The input optical power was set to 9 dBm and BER measurements were performed for data rates varying from 20 to 27 Gb/s

#202125 - $15.00 USD Received 28 Nov 2013; revised 12 Jan 2014; accepted 13 Jan 2014; published 24 Jan 2014

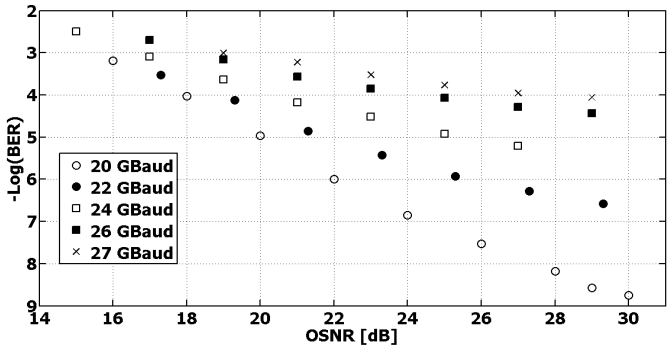

Fig. 6. BER vs. OSNR (resolution bandwidth = 0.1 nm) for varying data rate DBPSK signals.

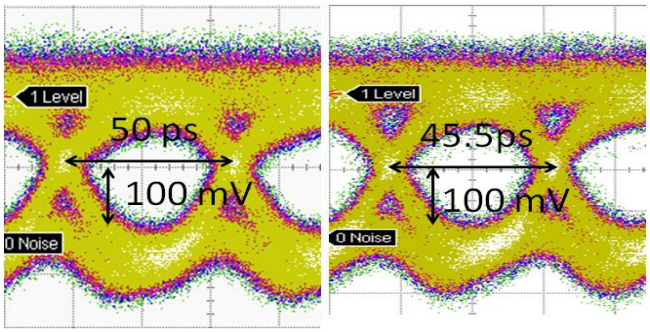

Fig. 7. Eye diagrams for (left) 20-Gbaud and (right) 22-Gbaud DBPSK signals.

as shown in Fig. 6. Here, TE-polarized light was coupled to one of the single-polarization grating couplers and the angle of the fiber was optimized for coupling efficiency. The angle of the fiber was approximately 80°. The PRBS length was 2^{31}-1. The performance degrades with increasing baud rate and this is due in part to electrical noise of the setup but primarily to the limited bandwidth of the photdetectors. Recall that the photodetector bandwidth is only 10 GHz, therefore the photodetectors are operating at a frequency well beyond roll over. The BER values are, however, below the forward error correction (FEC) limit (assumed to be $1x10^{-3}$). The penalties introduced for high data rates are due to the bandwidths of the MZI-DI and the balanced Ge photodetectors. Figure 7 reports the eye diagrams for 20- and 22-Gbaud DBPSK signals.

With the same measurement setup described in Fig. 5, the receiver was then characterized using DQPSK signals modulated at different baud rates and with a PRBS length of 2^7-1. Figure 8 shows the BER measurements vs. OSNR for 20 and 25 Gbaud received DQPSK signals for two orthogonal polarizations. The OSNR receiver sensitivity in order to have a BER = 10^{-9} is 35 dB at 20 GBaud. The plot in Fig. 8 indicates a clear BER floor near 10^{-5} for 25 GBaud, which is, well below the FEC limit. The performance penalty at 25 Gbaud is due

#202125 - $15.00 USD Received 28 Nov 2013; revised 12 Jan 2014; accepted 13 Jan 2014; published 24 Jan 2014

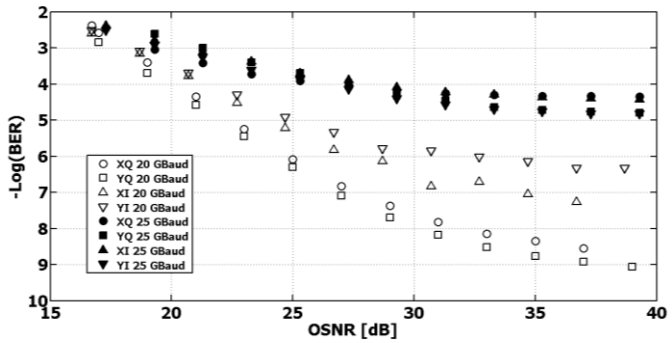

Fig. 8. BER vs. OSNR (resolution bandwidth = 0.1 nm) for 20 Gbaud and 25 Gbaud DQPSK signals.

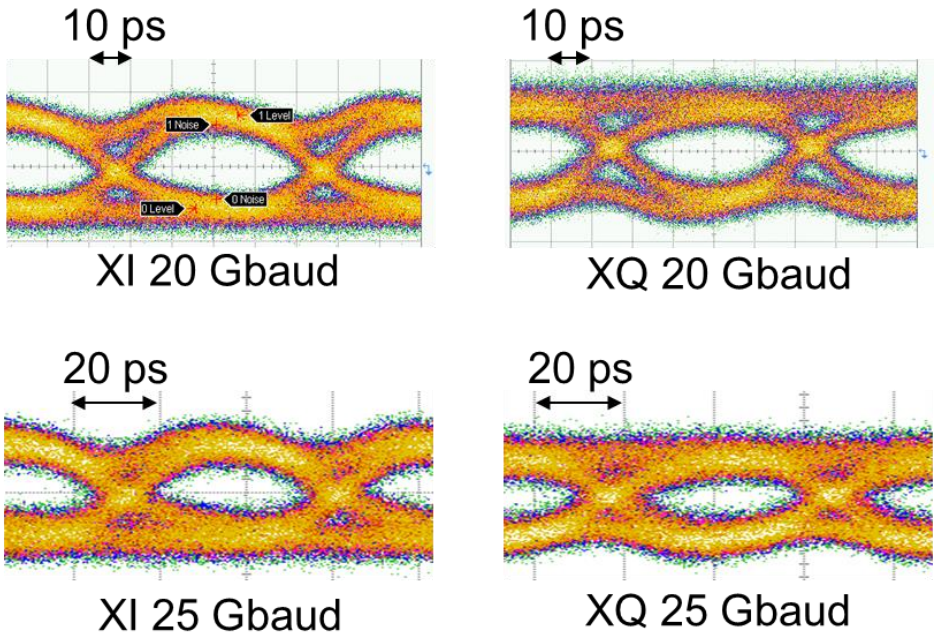

Fig. 9. Example eye diagrams for 20 Gbaud and 25 Gbaud signals.

primarily to the limited bandwidth of the individual photodetectors as well as the mismatch between the signal bit time and the bit delay of the DI, both of which could be improved in a future realization. For the 20 Gbaud data, there is a difference in performance for the I- and Q-channels, caused by an unequal splitting of the directional coupler splitters, which leads to a difference in the signal level incident of the balanced photodiodes. This affect is not observed at the higher baud rate (25 Gbaud) because the electrical noise of the amplifiers dominates. Eye diagrams of the two demodulated quadratures are shown in Fig. 9 for 20 and 25 Gbaud signals, demonstrated clear eye openings, with some degradation at 25 Gbaud relative to 20 Gbaud. Figure 10 shows the resampled constellation diagrams of two orthogonal polarization signals at 20 Gbaud monitored by a real-time oscilloscope.

#202125 - $15.00 USD Received 28 Nov 2013; revised 12 Jan 2014; accepted 13 Jan 2014; published 24 Jan 2014

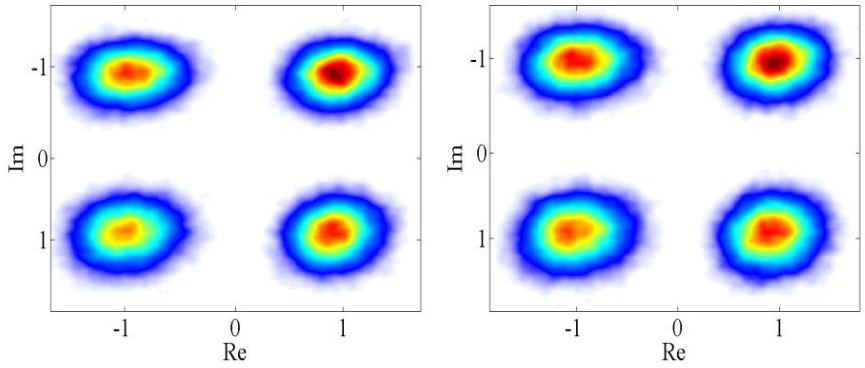

Fig. 10. 20-Gbaud signal constellation diagrams for (left) X polarization and (right) Y polarization.

4. Conclusions

An integrated Si receiver has been demonstrated for demodulation of PDM-DBPSK and PDM-DQPSK signals. The receiver consists of MZ-DIs for phase to intensity conversion and therefore employs noncoherent detection, which does not require arduous signal processing used for coherent detection or a local oscillator laser. Performance was demonstrated below the FEC limit for 25-Gbaud (up to 100-Gb/s) operation. Due to its simplicity relative to coherent detection, this receiver could extend the application space of such advanced modulation formats, namely PDM-DQPSK, to short- and medium-reach optical interconnects.

Acknowledgment

This work was partially supported by the Electrical and Computer Engineering Department at Boston University and by the Regione Toscana through the ARNO T3 project, POR CReO FESR 2007-2013, PAR FAS 2007-2013. The authors acknowledge OpSIS for foundry services and technical discussions and Pietro Contu for technical discussions.

#202125 - $15.00 USD Received 28 Nov 2013; revised 12 Jan 2014; accepted 13 Jan 2014; published 24 Jan 2014